Revista Brasileira de Física, Vol. 8, Nº 1, 1978

Some Pararneters Affecting the Minirnurn Diffracting Volume of the Back Reflection Line Kossel Patterns

JOEL REGUEIRA TEODOSIO and GUSTAU FERRAN

*Programa de Engenharia Metalúrgica e de Materiais, COPPE-Universidade Federal do Rio de Janeiro**

Recebido em 11 de Agosto de 1977

A very simple attachment has been fitted to a scanning Electron Microscope to produce back-reflection Kossel line patterns of selected diffraction areas. Although transmission, back reflection Kossel line patterns and pseudo-Kossel line patterns, have been obtained using the Electron Micro Probe Analyser, there are no reported experiments or recent theoretical studies concerning the minimum usable volume of the selected diffraction areas or the contrast of the patterns obtained. In the present paper, the authors studied some parameters affecting the contrast in the back-reflection Kossel line patterns, since such patterns provide information from smaller volumes than the pseudo - Kossel line patterns, where the x-ray source lies outside the sample. The parameters affecting the contrast here considered were: accelerating voltage, x-ray filter and grain perfection. In order to have a large number of grains and a wide range of diffracting areas, a partially recrystallized low carbon steel sheet was prepared. In this sample, 181 grains were selected to obtain Kossel line patterns. The analysis of the line contrast obtained using the back reflection Kossel line technique leads to the following conclusions: (i) it is possible to obtain dynarnic diffraction patterns from selected areas as small as 1.5 micrometers; (ii) photographs contain lines produced in volumes other than the selected one, but such lines can easily be identified, and (iii) there is a correspondence between the grain perfection observed metallographically and the diffracted lines sharpness and continuity.

* Postal address: C.P. 1191, 20.000 - Rio de Janeiro RJ.

Para produzir linhas de Kossel de difração de raios-x, a partir de áreas selecionadas, foi adaptado um simples acessório a um Microscópio Eletrônico de Varredura. Com o uso da Microsonda, já se tem obtido filmes de Kossel em reto-reflexão e transmissão, bem com filmes de pseudo-Kossel. Todavia, não existem trabalhos experimentais, ou estudos teóricos recentes, sobre o volume difratante ou o contraste das linhas obtidas. No presente trabalho, os autores estudam alguns parâmetros que afetam o contraste das linhas de Kossel em retro-reflexão. Essas linhas fornecem informações de menores volumes difratantes que as linhas de pseudo-Kossel, onde a fonte de raios-x localiza-se fora da amostra difratante. Os parâmetros que afetam o contraste e que foram aqui considerados são: voltagem de aceleração, filtro de raios-x e perfeição do grão difratante. Para obter um grande número de grãos e uma larga faixa de áreas difratantes, foi utilizada uma amostra de aço baixo carbono parcialmente recristalizado. Nessa amostra, foram selecionados 181 grãos, e obtidos os filmes de Kossel. A análise do contraste obtido fazendo-se uso da técnica de Kossel em retro-reflexão, conduz às seguintes conclusões: (i) é possível obter-se linhas de difração dinâmica de áreas selecionadas, com 1,5 micra de diâmetro; (ii) os filmes contêm linhas produzidas em regiões adjacentes à área selecionada, mas essas linhas podem, todavia, ser facilmente identificadas; (iii) há uma correspondência entre a perfeição do grão observada metalograficamente e a continuidade e contraste das linhas de difração.

1. INTRODUCTION

The Electron Micro Probe Analyser (EMPA) has been used to obtain Kossel line patterns (Peters and Ogilvie[1], 1965; Maurice, Seguin and Tixier[2], 1971), most of them in transmission and a few in back-reflection (Bevis and Swindells[3], 1965). The EMPA was adopted in preference to the x-ray Microfocus, both because of availability and for the following reasons:

(i) the observation facilities (optical and scanning microscopy), in EMPA, are very helpful in selecting the diffraction areas;

(ii) the possibility of obtaining x-ray diffraction patterns from smaller volumes than can be obtained using the x-ray Microfocus unit; and

(iii) both Kossel and pseudo-Kossel line patterns are produced in EMPA instead of pseudo-Kossel line patterns only.

The users of the EMPA technique generally agree that it is possible to measure lattice parameter and orientation from Kossel line patterns obtained on grains of an apparent diameter close to 10 micrometers; however, to the authors' knowledge there are very few reports of experiments or recent theoretical work concerning the minimum volume of the selected areas that provides this type of diffraction pattern. There are only the early experimental work by Voges and Kossel[4] (1935), and Von Laue's dynamical calculation of the line intensities, summarized in James'[5] book (1962), concerning the minimum volume of the selected areas.

In the present paper, the authors report some results acquired in a systematic survey of the Kossel line patterns contrast, obtained on a polycrystalline specimen. The diffraction patterns were obtained from the specimen at the beginning of recrystallization (less than 10% volume fraction recrystallized), with the aim of finding the orientation distribution of the new grains and to have a better understanding of the texture formation by grain growth (Teodósio and Ferran[6] 1975). Most of the patterns were obtained in a scanning electron microscope (SEM), which has a satisfactory resolution for observing and selecting diffraction areas.

2. EXPERIMENTAL METHODS

2.1. Kossel Attachment

A very simple attachment has been fitted to the SEM Stereoscan Mark II, to record back-reflection Kossel line patterns produced on small areas of the specimen. The diffracting areas were selected using the scanning imaging system, while x-ray film blackening has been avoided during this observation period by using a remvable shutter.

A short specimen-film distance - 1.9 cm - was used:
(i) to decrease exposure time; (ii) to record the patterns with a large solid angle (π radian) and (iii) to have a working distance in the SEM (2.9 cm) that nevertheless allows of good image resolution without any modification of the lenses.

A single-coated x-ray film with fine grain size was adopted (Kodak single R) to see fine details in the diffraction patterns. Typical exposure times at 2.5 × 10^{-8} Amps using a thin, 12.5 micrometers, iron foil filter, were 18 minutes at 16 kV, and 5 minutes at 28 kV, for grains larger than 6 micrometers.

2.2. Sample Characteristics

The sample was a low carbon (0.03%) steel sheet, previously cold rolled 68% and then partially recrystallized. Using the point counting technique over 185 subareas (Underwood[7] 1968), the volume fraction of recrystallized material was estimated to be 8%. Figure 1, taken in a region of new grains, labelled by N, shows a typical metallographic view of the specimen: the new grains are grouped, forming colonies and are surrounded by a recovered matrix with a corrugated appearance R, and no recovered matrix with flat surface, D.

A linear grain-size distribution was obtained (Figure 2, step curve 2) by measuring individually the diameter of 1500 new grains on a plane section of the sample. Since the diffraction occurs within the volume and the diameters measured on a plane section are smaller or equal to the corresponding grain volume diameter, the two dimensional grain size distribution was transformed to a three dimensional one (Figure 2 curve 1) using the method proposed by Saltykov and described by Underwood[7] (1968). Such a sample offers a wide range of diffracting areas (from 1 to 20 micrometers approximately) and furthermore contains a large number of grains.

2.3. Accelerating Voltage

The accelerating voltage, for the electrons used to produce x-rays, plays an important role in the back-reflection Kossel line contrast. Since this parameter has not received very much attention - only Yakowitz[8] (1966) considered its effects on the transmission Kossel line patterns - we shall make some comments about penetration depth and lateral resolution, and the relative intensity of both characteristic line and white radiation spectra. The effective electron range z, representing the maximum depth still producing characteristic x-ray emission by incident electrons, depends for

a given material on the accelerating voltage. Theoretical expressions for z can be obtained by integration of the Bethe energy loss formula. The expression usually used in microanalysis is due to Castaing[9] (1960):

$$z = 0.033 \, (E^{1.7} - E_c^{1.7}) \, \frac{A}{\rho Z} \, ,$$

where E is the accelerating voltage, E_C the excitation voltage to produce a characteristic line (both in kV), A the atomic weight, Z the atomic number, and ρ the density. Another expression, due to Reed[10] (1966), indicating the depth within which 99% of the total x-ray characteristic radiation production takes place, is

$$z = 0.077 \, (E^{1.5} - E_c^{1.5}) \, \frac{1}{\rho} \, .$$

In Table 1, values of z (in micrometers) were calculated, for iron, at several accelerating voltages. Furthermore, the experimental data of the lateral spreading measured by Russ and Kabaya[11] (1969) in a SEM are included, showing much smaller values. These measured data were determined with a beam current of 10^{-12} Ampère. Table 1 shows the advantage of working at low accelerating voltages: the maximum depth of the x-ray source is smaller and the white radiation should decrease; this latter effect is more important in back-reflection Kossel lines than in transmission, where there is an important self filtering effect.

Lateral spreading, D, is defined usually as $D = d + z$, where d is the beam diameter, and z the effective penetration depth. When the beam current is small, the beam diameter reaches small values and the lateral spreading measured by Russ and Kabaya[11] is close to the penetration depth z. To decrease d, one possibility is to increase the accelerating voltage, E, keeping the electron beam current, i_m, constant, as shown in the relation

$$i_m = \text{Const.} \times E \, d^{8/3} \, ,$$

but then, as was shown earlier, z increases. Another possibility is to decrease i_m, keeping E constant. The limitation to this is the decrease of x-ray intensity production, since the film exposure time is directly proportional to the beam current, all the other parameters being constant.

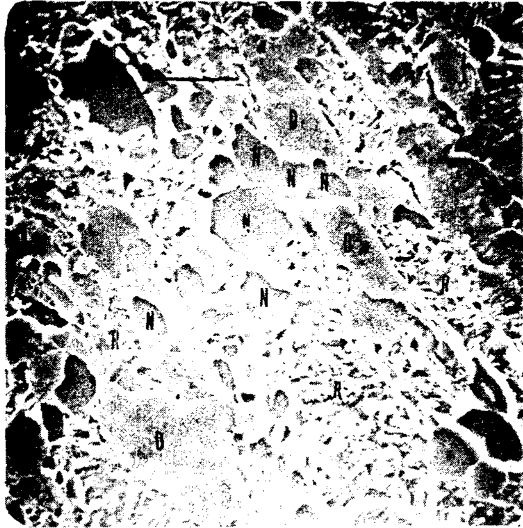

FIG.I - Scanning Electron Micrograph of the partially recrystallized iron sample (segment length 16 micrometers), N new grain, R recovered matrix.

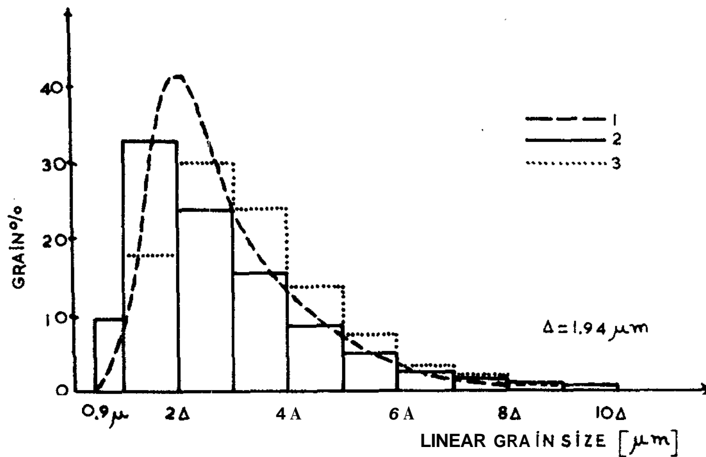

FIG.2 - Grain size distribution for 1500 grains. (1) Three dimensional;(2) Two dimensional; (3) Two dimensional, on 181 diffraction patterns.

Furthermre, during long exposure times (t > 10 minutes) beam shift sometimes occurs and the pattern is useless.

Finally, the accelerating voltage cannot decrease too much in the SEM, because its resolution degrades rapidly, specially at long working distances such as 2.5 cm. In the present case, E was kept at least at 14 kV.

Accelerating Voltage	12 kV	14kV	16kV	18kV	25 kV	30 kV
CASTAING (1960)	0.38	0.58	0.80	1.03	2.35	2.80
REED (1960)	0.22	0.32	0.43	0.56	1.02	1.44
RUSS & KABAYA (1969) Experimental	0.3					0.8

TABLE 1. Effective electron penetration range z (microrneters), in iron, at several accelerating voltages.

G (%)	$\frac{1}{\mu} \ell n \frac{1}{1-G}$	$\phi = 25^o$		$\phi = 15^o$		$\phi = 5^o$		$\phi = 0^o$	
		x	y	x	y	x	y	x	y
99	80.4	4.5	77.9	14.0	73.2	18.6	71.0	19.1	70.6
50	11.7	0.7	11.7	2.1	10.9	2.8	10.7	2.9	10.6
20	3.9	0.2	3.8	0.7	3.5	0.9	3.4	0.9	3.4

TABLE 2. Normal (x) and lateral (y) paths within the sample, necessary to produce a fraction G of the total diffracted intensity, for several values of ϕ (units in micrometers).

3. DIFFRACTION PATTERNS OBTAINED: RESULTS AND DISCUSSION

3.1. Patterns Obtained

The selected areas for diffraction experiments (new grains N in Figure 1) were chosen between the lower limit (0.9 micrometers) and the upper limit (20.3 micrometers) for a 1500 grains distribution, but the smaller number of grains studied (diffraction patterns obtained - 181) did not reach such limits. The diameter of the minimum area producing a diffraction pattern was of 1.5 micrometers. In Figure 2, the step distribution 3 represents the grain size distribution of the 181 diffracting areas.

The set of diffraction conics expected from the Bragg law and the structure factor are: 12 reflections of type {110}, 6 of type {200}, 24 of type {112} and 12 of type {220} for each wavelength of iron $K\alpha_1$, $K\alpha_2$ and $K\beta$, but no $K\beta$ pattern was observed.

The non-recrystallized fraction of the specimen showed two different morphologies:
(i) areas with corrugated appearance produced only one or two {110} ellipse portions and they were classified as recovered matrix R, as shown in Figure 1; (ii) flat areas of irregular shape, D, did not produce any diffraction pattern and they were classified as non-recovered matrix.

In the set of 181 photographs obtained on new grains, all of them had diffraction lines. The better contrast (or signal-to-noise) ratio, is shown by some {110} lines, followed by {220}, {112} and {002} in order of decreasing contrast; lines {110} appear in every film, but not always the other lines.

Figure 3 shows schematically the relative position of the x-ray source, diffracting plane and specimen surface, where S represents an x-ray point source. Actually, the ionization of the L shell takes place between the specimen surface, excluding a thin layer where there is elastic scattering and the point, S, at a depth of the order of the penetration range z. When ϕ, the angle between the specimen surface and the diffracting planes, is smaller than the Bragg angle 0, the patterns obtained are ellipses or cir-

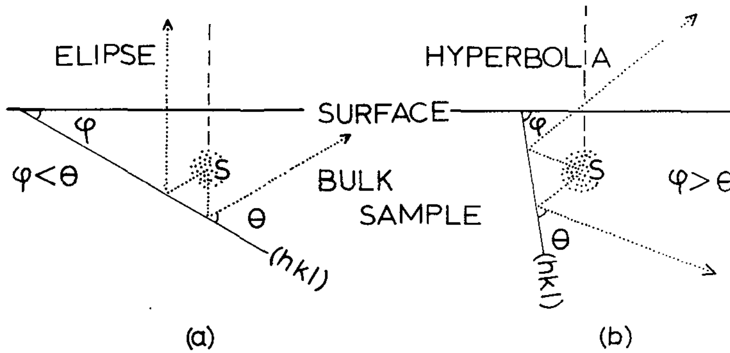

FIG.3 - Relative positions of X-Kay source and diffracting plane back-reflection Kossel line patterns: (a) ellipses and circles $\phi < 0$; (b) hyperbolas $\phi > \Theta$.

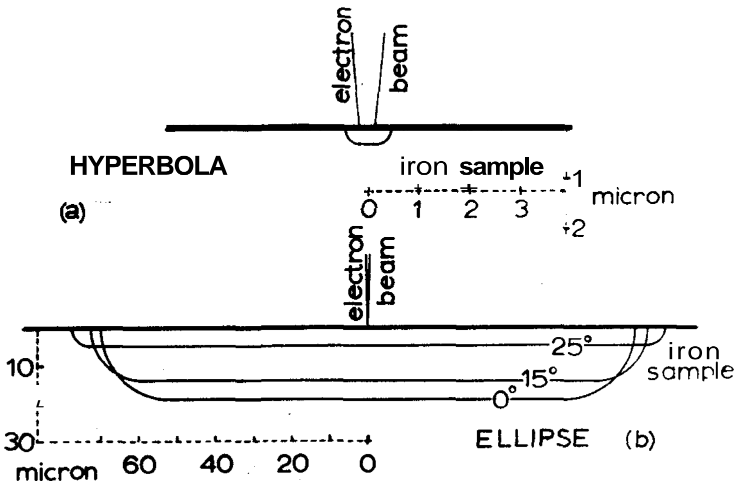

FIG.5 - Production limits of back-reflection Kossel line patterns shown schematically for (a) hyperbolas $\phi > 0$; (b) ellipses or circles $\phi < \Theta$, + film center (see Table 2).

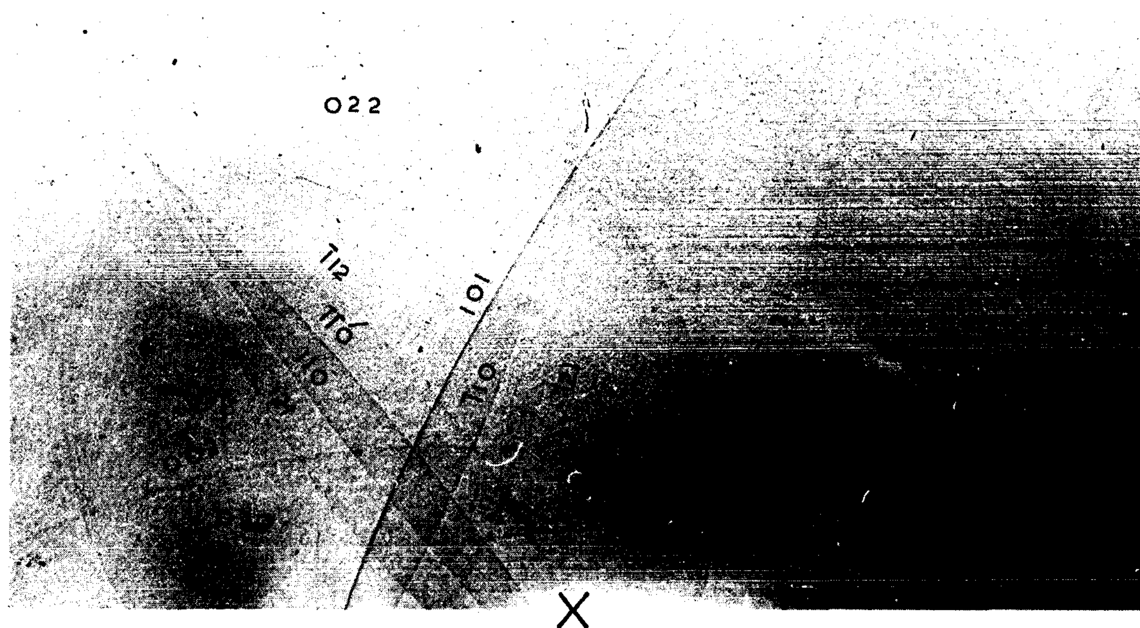

FIG.4 - Detail of a back-reflection Kossel line pattern (segment length 10 millimeters) with the same contrast as the original film.

cles ($\phi = 0$) (Figure 3a). In back reflection technique when $\phi > 0$, hyperbola lines are recorded only if the x-ray source is within the specimen. As shown in Figure 3b, the diffraction volume is limited by the surface of the specimen and the source S. In these experiments, the depth of the point S should be: $0.3 < z < 0.8$ micrometers, as was shown in Table 1 for accelerating voltage of 16 kV.

The {110} hyperbolas represent 80% of the whole number of recorded {110} patterns. This large number of hyperbolas can be explained considering the Bragg angle for the {110} diffraction - 28.5° - and the geometrical limitations of the film holder, that only produces visible iron patterns for $96^{\circ} > \phi > 13^{\circ}$. Such conditions reduce the recorded ellipse patterns to the range of $28.5^{\circ} > \phi > 13^{\circ}$, while the {110} hyperbolas can appear in the range $96^{\circ} > \phi > 28.5^{\circ}$. So, the ratio of the angular range available for hyperbolas to the whole angular range $(96^{\circ} - 28.5^{\circ})/(96^{\circ} - 13^{\circ}) = 81\%$ is very close to the observed fraction.

3.2. Pattern Contrast

Figure 4 is a film portion showing the diffraction patterns indexed. The ellipse {101} is the more intense one, while the hyperbolas $\{\bar{1}10\}$, $\{\bar{1}\bar{1}0\}$ and {110} of the same family of planes are much weaker. This difference in intensity depends on the relative position of the x-ray source, diffracting plane and specimen surface as shown on Figure 3. Contrary to the Kossel and Voges[4] (1935) remark, the observed hyperbolas are not more intense or sharper than the ellipses; furthermore, on the recorded patterns, the intensity of both conics decreases with increasing values of ϕ.

Considering, in Figure 3, another specimen surface through the point Sand parallel to the first one, the hyperbola produced in Kossel back - reflection can be compared - as a rough approximation - to diffraction through a crystal plate (LAUE case). For such a geometrical setting, the plate thickness giving the maximum intensity for mosaic crystals is $t = \cos \phi/\mu$ (James[12], 1962) when $\phi = \pi/2$, and in the present case t (110) = 15 micrometers.

At this point, it is worttiwhile to give the primary extinction distance ε (110) = 0.38 micrometers, that was estimated from the relation

$$(\varepsilon)^{-1} = \bar{\tau} = \frac{\pi}{2} \frac{e^2}{mc^2} N\lambda \, |F| \, ,$$

where $\bar{\tau}$ is the average attenuation coefficient in the middle region for a perfect crystal set in the reflecting position (Warren[13], 1968), N the number of atoms per unit of volume, λ the wave length and F the structure factor. Since t (110) >> $z \simeq \varepsilon$ (110), the hyperbola intensity recorded cannot be explained by the kinematical theory but only by the dynamical theory for perfect crystals. Since the irradiated volume in the hyperbola case is so small, in such a region the crystal may be perfect.

Although Figure 3 shows schematically that the diffracting volume responsible for production of ellipses is beneath the point S, it is of interest to have a quantitative estimation of the volume producing a given fraction, G, of the diffracted intensity for mosaic crystals, as it was done for hyperbolas. The following relation, due to Cullity[14] (1959), .

$$x = \frac{1}{\mu} \, \ell n \frac{1}{1 - G} \cdot | \text{ cosec } (\Theta - \phi) + \text{cosec } (\Theta + \phi) |^{-1} \, ,$$

gives the penetration depth, x, normal to the surface; this relation leads to the conclusion that the path length within the diffracting volume is $(1 - \mu) \, \ell n [1/(1-G)]$, independently of the Θ and ϕ values. The path component parallel to the surface is

$$y = \frac{1}{\mu} \, \ell n (\frac{1}{1 - G}) \frac{\cos \Theta}{\cos \phi} \, .$$

Table 2 gives values of x and y (in micrometers) for iron, reflection {110} ($\Theta = 28.5^{\circ}$), calculated for several values of G and ϕ ($\phi < 0$ for ellipses). Table 2 shows that x changes rapidly with ϕ but not y, for a fixed value of G. Considering that the average grain diameter is 5.1 microns, the x and y values on this Table show that the kinematical theory could account, on the average, for less than 20% of the ellipses intensity. Thus, the diffracted intensity of ellipses must be explained by the dynamical theory of diffraction. There is a further observation requiring the dynamical theo-

ry to be understood: the convex side of the lower intensity ellipses and hyperbolas is clearer than the adjacent background.

3.3. Minimurn Diffracting Volume

A noteworthy observation was the presence of {110} ellipses, that could not be indexed coherently with other lines $\{hk\ell\}$ already indexed in the same film, because their measured interplanar angles differed from the correct crystallographic values. The "non-indexed" {110} lines, present in many films, may be diffracted from grains adjacent to, or beneath, the selected areas as explained in the following paragraph.

The man grain size masured is 5.1 micrometers (5.1×10^{-4} cm) and the mass absorption coefficient of iron for Kα radiation of iron is 510 cm^{-1}; the photoelectric law of absorption, $I/I_0 = \exp(-\mu x)$, for such data shows that the generated x-rays still keep 75%of their original intensity after going through the average recrystal1ized grains on the sample surface. Consequently, diffraction by the x-rays still available will originate continuou-ellipses when the material is recrystallized, broken ellipseswhen the material is recovered, and no lines at all when the material is not yet recovered, such material being located in each case beneath or around the selected areas.

It was also observed that 19 photographs were not showing {110} hyperbolas, but showing some {110} ellipse lines running over the whole film or a portion of it. Following the arguments given above, one can assume that the 19 patterns, without {110} hyperbolas but with some {110} ellipses, either originate from regions beneath the selected areasor that there was some electron beam shift during the exposure.

After this analysis of the Kossel line patterns was obtained, there wasno problem in recognizing the diffracted lines: those {110} hyperbolas and other {110}, {220} ellipses associated with them, making the correct interplanar angle, originated in the selected area. The basis in establishing such correspondence lies in the fact that {110} hyperbolas only originate at a depth smaller than 0.8 micrometers (Table 1). The other ellip-

ses {110}, {112} and {220} - incompatible with the {110} hyperbola - should come from regions adjacent to the selected areas.

The results obtained after studying the back-reflection Kossel line patterns on a partially recrystallized iron are summarized schematically on Figure 5: the {110} hyperbolas are formed only on a thin layer beneath the surface, the depth of which depends on the penetration range z, and it is drawn in Figure 5 for 16 kV.

The {110} and also the {112}, {220} and {200} ellipses ($\phi > \Theta$), may originate at a depth of the order of z (dynamical patterns) or $1/\mu$, as shown in Table 2, if the grains are large enough; in the latter case the line width would be larger.

Figure 5 also shows that the lateral resolution for the production of {110} dynamic patterns is poorer than the depth resolution, which is of the same order as the quantitative resolution defined by Reed (1966) for electron microprobe analysis, neglecting fluorescence. In the present experiments, the lateral resolution is between 1.5 and 2 micrometers, at 16 kV and 1.0×10^{-8} Amps.

It is now possible to discuss the reasons why recrystallized iron grains of apparent sections smaller than 1.5 micrometers did not produce any sort of diffraction patterns. (i) This could be related to the poor lateral resolution and beam shift;, centering the 0.3 micrometers diameter beam would let roughly 0.8 micrometers at each side of the beam, for having dynamic diffraction when $\phi \simeq 90^{0}$; furthermore, any small beam shift would make it very difficult to obtain such diffraction patterns. (ii) The next explanation is related to the penetration depth of electrons: as it was calculated and measured, one did not take into account the possibility of electron channelling; in the present experiments, the new grains are nearly perfect and consequently the ionization of $K\alpha$ in iron at 16 kV could occur still further down than 0.8 micrometers by electron channelling. (iii) Another related point could be the fact of not taking into account the secondary fluorescence yield of $K\alpha$ radiation, that is produced deeper than the effective electron penetration range, but with the small overvoltage utilized ($E/E_c \simeq 2.2$) one would not expect an important contribution. The

final reason (iv) is to consider that two extinction distances are not enough to produce observable dynamic diffraction with the present experimental settings.

The authors are pleased to acknowledge a valuable discussion with Prof. Kasutake Kohra. We gratefully acknowledge the financial support from CNPq and BNDE.

REFERENCES

1. Peters, E.T. and Ogilvie, R.E., Trans. AIME 223, 89-95 (1965).
2. Maurice, F., Seguin, R. et Tixier R., "Determination Precise du Paramètre Cristallin au Moyen des Diagrammes de Difraction en Faisceaux X Divergents", 6th International Congress on X-Ray Optics and Micro-Analysis (Osaka, Japan, 1971).
3. Bevis, M. and Swindells, G., Phys. Stat. Sol. 20, 197-212 (1967).
4. Kossel, W. Von, and Voges, H., Ann. der Physik, 5 fol., *23*, 677-704 (1935).
5. James, R.W., *The Optical Principles of the Diffraction of X-Rays,* Chap. VII (London, Bell and Sons, 1962).
6. Teodosio, J.R. and Ferran, G., *"Use of the Kossel Technique to Study the Primary Recrystallization Texture in Low Carbon Steel"*, 4th European Colloquium on Textures (Cambridge, England, 1975).
7. Underwood, E.E., *Quantitative Microscopy,* Chap. 6, 162-168, Editors: De Hoff and Rhines (McGraw Hill, New York, 1968).
8, Yakowitz, H., J. Appl. Phys. 37, 4455-4458 (1966).
9. Castaing, R., *Advances in Electronics and Electron Physics,* 317-325; Editor: L. Marton (Academic Press, N. York, 1960).
10. Reed, S.J.B., 4 *th International Congress on X-Ray Optics and Micro-Analysis.* Editors: Castaing, Deschamps et Philibert (Hermann, Paris, 1960).
11. Russ, J.C. and Kabaya, A., *Proceedings of the 2nd Annual Scanning Electron Microscope Symposium,* 59-61; Editor: Ohari (Chicago: ITT Research Institute, 1969).
12. James, R.W., Loc. cited, Chap. 2, p. 46.
13. Warren, B.E., *X-Ray Diffraction,* Ch. 14 (Addison-Wesley, London, 1968).
14. Cullity, B.D., *Elements of X-Ray Diffraction,* Ch. 9-5, (Addison Wesley, London, 1959).